VETOMAC VIII International Conference
On Vibration Engineering And Technology of Machinery
Gdansk, Poland, 2012
Paper Number: VM2012-10014

MODELLING OF MULTILAYERED VISCOELASTIC ROTORS – AN OPERATOR BASED APPROACH

H.Roy[1], J.K. Dutt[2*], S.Chandraker[3]
[1,3] Department of Mechanical Engineering
National Institute of Technology, Rourkela-769008, Orissa, India

[2] Department of Mechanical Engineering
Indian Institute of Technology, Delhi, New Delhi - 110016, India

Key words: Viscoelastic multilayered rotor, Viscoelastic Internal damping, Anelastic displacement field, Stability limit of polymeric rotors.

Abstract: This paper presents a study of the dynamic behavior of a multilayered viscoelastic rotor-shaft system, where the material damping in different layers of the rotor shaft introduces rotary dissipative forces well known to cause instability of the rotor-shaft system. For the sake of modelling, material constitutive relationships of different layers are represented in the time domain with the help of Differential time operators and Anelastic Displacement Field (ADF) variables as this combination enables easy representation of general linear viscoelastic behaviour. Equations of motion of a rotor-shaft system are obtained in time domain after discretizing the shaft-continuum by using finite beam elements. The equations thus developed have been used to find the stability of a rotor-shaft system in terms of Stability Limit of spin-Speed (SLS) as well as the frequency response when the rotor-shaft-system is subject to dynamic forcing due to disc-unbalance. Effect of thickness and placement of viscoelastic layers is studied numerically for a 2-layered, 2-disc simply supported rotor-shaft system for an example.

1 INTRODUCTION

Unlike elastic materials, the viscoelastic materials store energy and also dissipate it when subject to dynamic loading. For this reason, viscoelastic materials are extensively used for vibration control; [1] has reported many such applications.

Tangential forces in rotor shaft systems e.g. due to shaft material damping, friction forces between disc and shaft in built-up rotors, fluid film forces, steam induced forces etc. play an important role to decide dynamic behaviour of rotors.

[1] Assistant professor, Email – hroy77@rediffmail.com Telephone: 91-661-2462526
[2] Professor, E-mail – jkrdutt@yahoo.co.in, Telephone: 91-11-26596334
3Research Scholar, Email – saurabh01anizer@gmail.com Telephone: 91-9861941006
* Corresponding Author (email - jkrdutt@yahoo.co.in)

Unlike in structures, spin of rotors introduces rotary damping force or forces, that act tangential to the rotor orbit, and is well known to cause instability in rotor-shaft systems after certain spin speed. Thus, a reliable model considering all sources of tangential forces is indeed necessary to represent the rotor internal damping for correct prediction of stability limit of spin speed of a rotor-shaft system. However this work concentrates on studying the effect of tangential force due to viscoelastic shaft material damping on the dynamics of a multilayered viscoelastic rotor-shaft system, which is light, sufficiently stiff and is good for cold operating environment.

Viscous and hysteretic damping models were used by a number of researchers e.g. [5],[6],[7] to take into account the frequency dependent and independent portions of energy dissipated for representation of shaft material damping. Voigt model (2-element model) was used to represent the shaft material constitutive relationship by [8],[9] who discretized shaft continuum using finite beam elements to derive equations of motion and study dynamic behaviour of rotor-shaft systems.

However both viscous and hysteretic damping models are unsuitable for proper representation of viscoelastic material behaviour. In viscoelastic materials, stress and strain are not generally in phase under dynamic deformation, the frequency of which for cyclic deformation has considerable influence on energy storage and dissipation. For this reason, in linear viscoelastic solids, the instantaneous stress is obtained by operating the instantaneous strain by the modulus operator $E(\ )$, a function of differential time operators; the function being a constant (the Young's modulus) for the special case of linear elastic behaviour. Different multi-element spring-damper models [2] like the 2, 3, 4 element models as well as internal variable models e.g. Augmenting Thermodynamic Field (ATF) by [3] and Anelastic Displacement Field (ADF) by [4] are used to represent the operator and also the constitutive relationship of linear viscoelastic material.

Of few authors reporting viscoelastic rotor models for studying the dynamic behaviour of rotors are the reports by [10],[11],[12], where authors of the first used a 3-element material model and the authors of the latter used ATF approach respectively for the constitutive relationship and studying dynamic behaviour of a viscoelastic rotor-shaft system discretized with finite beam elements. Recently [13] used a generic operator based approach to represent the constitutive relationship and derive the equations of motion of viscoelastic rotor-shaft system after discretizing the shaft continuum by finite beam elements. While all the approaches (multi-element, ATF, ADF) are essentially the same, yet the mathematical advantage of using a generic operator approach is that it may be suitably tailored according to the material constitutive relationship to obtain the equations of motion in time domain.

The importance of multi-viscoelastic layers arises from using the stiffness, damping and specific gravity of different elastomeric materials for tailoring the dynamic behaviour of a rotor-shaft system. The multilayered rotor-shaft is assumed to be made of a number of perfectly bonded linear viscoelastic layers of several

materials. The instantaneous stress for different layers is obtained by operating the instantaneous strain by a linear differential time operator. The ADF approach is used for writing the constitutive relationships and next the differential time operator, where the coefficients of the operator are formed by ADF parameters are used to write the equations of motion of a rotor-shaft system after discretizing the continuum using finite beam element.

For an example, the equations of motion of a 2-layered, 2-disc simply supported rotor shaft system has been derived and the same has been used to obtain the eigenvalues numerically for studying stability limit of the spin speed as well as the Campbell Diagram. The equations of motion are further used to study the unbalanced vibration response within the stable zone of spin speed. The effect of placement of layers as well as their ratio of thicknesses is also studied for getting an idea of maximizing the stability limit speed as well as the first critical speed.

2 CONSTITUTIVE RELATIONS

The constitutive relationship for each layer is assumed to be represented by a single ADF (Anelastic Displacement Field) and obtained from the Helmholtz free energy density function, $\mathcal{H}$ representing a thermodynamic potential, where the total strain is the sum of elastic strain and the anelastic strain. The Helmholtz free energy for j^{th} layer is given by equations (1) after following [4] and corresponding material constitutive relations are given by equations (2).

$$\mathcal{H}_j = \frac{1}{2}\left(E_j \varepsilon^2 - 2E_j \varepsilon \varepsilon_j^A + E_j^A \varepsilon_j^{A^2} \right) \tag{1}$$

$$\sigma_j = \frac{\partial \mathcal{H}_j}{\partial \varepsilon} = E_j \left(\varepsilon - \varepsilon_j^A \right) \tag{2a}$$

$$\sigma_j^A = -\frac{\partial \mathcal{H}_j}{\partial \varepsilon_j^A} = E_j \left(\varepsilon - C_j \varepsilon_j^A \right) \tag{2b}$$

In the preceding equations, E is the elastic modulus, σ is the total stress, ε is the total strain, σ^A is the anelastic stress, ε^A is the anelastic strain, E^A is the anelastic material property and $C = \dfrac{E^A}{E}$ is a coupling parameter. j represents the j^{th} layer

The relaxation equation (ref.[4]) for jth layer is written as

$$\dot{\varepsilon}_j^A + B_j \varepsilon_j^A = \frac{B_j}{C_j} \varepsilon \tag{3a}$$

or,

$$\varepsilon_j^A = \frac{B_j}{C_j} \frac{1}{B_j + \mathrm{D}} \varepsilon \tag{3b}$$

where B_j is the inverse of relaxation time for the j^{th} layer and $\mathrm{D}=d/dt$. Putting the value of ε_j^A from (3b) in (2a), the constitutive relationship is rewritten as

$$\sigma_j = E_j\left(1-\frac{B_j}{C_j}\frac{1}{B_j+\mathrm{D}}\right)\varepsilon = \mathrm{E}_j(\ )\varepsilon \tag{4}$$

where the modulus operator $\mathrm{E}_j(\ ) = \dfrac{a_{0_j} + a_{1_j}\mathrm{D}}{b_{0_j} + b_{1_j}\mathrm{D}}$, $a_{0_j} = E_j B_j\left(1-\dfrac{1}{C_j}\right)$, $a_{1_j} = E_j$, $b_{0_j} = B_j$, $b_{1_j} = 1$.

It may be seen that the time operator portion of E ( ) yields a non-zero value only if the strain is dynamic and gives rise to dynamic stress.

3 FINITE ELEMENT FORMULATION

The finite element model of the viscoelastic rotor shaft system is based on the Euler-Bernoullie beam theory. A beam element of length 'l' with nodal displacement variables is shown in fig. 1. Mechanical and anelastic displacements are denoted by q_{iy}, q_{iz}, (i = 1 to 4) and p_{kz}, p_{kz} (where k = 1 to 2) respectively, where p_{ky}, p_{kz} are the coordinates showing the internal variable (single ADF).

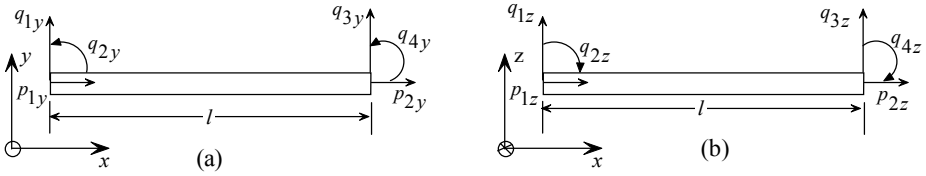

Fig. 1 A damped beam bending element showing the nodal displacements of two fields

The displaced cross-section of a multilayer rotor-shaft at any distance 'x' from the left end is shown in fig. 2, where different layers have been shown with different colours. The inner and outer radius of the j^{th} layer are r_{i_j} and r_{o_j} respectively. Coordinates of the shaft centre at any instant of time,'t', are given by the coordinates ($v(x,t)$, $w(x,t)$) along 'y' and 'z', the transverse directions respectively, where 'x', 't' are the spatial and temporal variables. Angle'Ωt' denotes the instantaneous orientation of the radius vector which is the instantaneous deflection $R(x,t)$, shown in the fig. 2 as 'R' for convenience. An infinitesimal element, of thickness 'dr', subtending an angle '$d(\Omega t)$' at the centre, chosen at a radius 'r' and angular location 'Ωt', where 'Ω' and 'ω' denote respectively the spin and whirl frequencies of the rotor in radians per second.

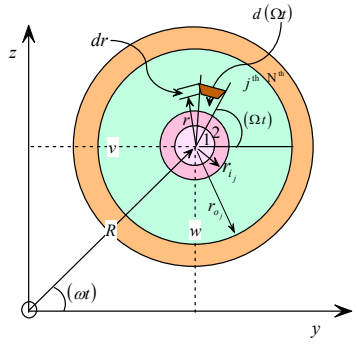

Figure 2: Displaced position of the shaft cross-section

The mechanical strain ε_x induced in the infinitesimal element in the 'x' direction is expressed after following [8] as

$$\varepsilon_x = -r\cos\left[(\Omega-\omega)t\right]\frac{\partial^2 R(x,t)}{\partial x^2} \tag{5}$$

Following [8] the bending moments at any instant of time about the y and z-axes are expressed as

$$\begin{aligned} M_{zz} &= \int_0^{2\pi}\int_0^{r_o} -\left(v + r\cos\left(\Omega t\right)\right)\sigma_x r dr d(\Omega t) \\ M_{yy} &= \int_0^{2\pi}\int_0^{r_o} \left(w + r\sin\left(\Omega t\right)\right)\sigma_x r dr d(\Omega t) \end{aligned} \tag{6a}$$

Substituting σ_x from equation (4) in the expressions for bending moment (equations (6a)) and utilizing the expressions of ε_x in equation (5), the expression for bending moments for N layered rotor are rewritten as

$$\begin{aligned} M_{zz} &= \sum_{j=1}^{N}\int_0^{2\pi}\int_{r_{i_j}}^{r_{o_j}} -\left(v + r\cos\left(\Omega t\right)\right)\frac{a_{0_j}+a_{1_j}\mathrm{D}}{b_{0_j}+b_{1_j}\mathrm{D}}\left[-r\cos\left(\Omega t-\omega t\right)\frac{\partial^2 R(x,t)}{\partial x^2}\right] r dr d(\Omega t) \\ M_{yy} &= \sum_{j=1}^{N}\int_0^{2\pi}\int_{r_{i_j}}^{r_{o_j}} \left(w + r\sin\left(\Omega t\right)\right)\frac{a_{0_j}+a_{1_j}\mathrm{D}}{b_{0_j}+b_{1_j}\mathrm{D}}\left[-r\cos\left(\Omega t-\omega t\right)\frac{\partial^2 R(x,t)}{\partial x^2}\right] r dr d(\Omega t) \end{aligned} \tag{6b}$$

After performing the integrations, it can be rewritten as

$$\begin{Bmatrix} M_{zz} \\ M_{yy} \end{Bmatrix} = \left[\begin{bmatrix} \sum_{j=1}^{N}\frac{a_{0_j} I_j}{b_{0_j}+b_{1_j}\mathrm{D}} & \sum_{j=1}^{N}\frac{a_{1_j} I_j}{b_{0_j}+b_{1_j}\mathrm{D}}\Omega \\ \sum_{j=1}^{N}\frac{a_{1_j} I_j}{b_{0_j}+b_{1_j}\mathrm{D}}\Omega & \sum_{j=1}^{N}-\frac{a_{0_j} I_j}{b_{0_j}+b_{1_j}\mathrm{D}} \end{bmatrix}\begin{Bmatrix} v'' \\ w'' \end{Bmatrix} + \begin{bmatrix} \sum_{j=1}^{N}\frac{a_{1_j} I_j}{b_{0_j}+b_{1_j}\mathrm{D}} & 0 \\ 0 & \sum_{j=1}^{N}-\frac{a_{1_j} I_j}{b_{0_j}+b_{1_j}\mathrm{D}} \end{bmatrix}\begin{Bmatrix} \dot{v}'' \\ \dot{w}'' \end{Bmatrix}\right] \tag{6c}$$

where, I_j is the area moment of inertia of j^{th} layer.

For the 2-noded finite beam element with 4 degrees of freedom per node the displacements v (x,t), $w(x,t)$ along and slopes $\Phi(x,t)$, $\Gamma(x,t)$ about 'y' and 'z' axes are given by equation (7), where the arguments 'x', 't' are dropped for convenience and $\{q(t)\}$ denotes the nodal displacement vector.

$$\begin{Bmatrix} v \\ w \end{Bmatrix} = \left[\phi(x)\right]^T \{q(t)\}; \; \Phi = -\frac{\partial w}{\partial x}; \qquad \Gamma = \frac{\partial v}{\partial x} \tag{7}$$

The differential bending energy is given by $dP_B^e = \frac{1}{2}\begin{Bmatrix} \Gamma' \\ \Phi' \end{Bmatrix}^T \begin{Bmatrix} M_{zz} \\ M_{yy} \end{Bmatrix}$ and may be integrated over the length of the element to obtain the expression of the total bending energy, which comprises strain energy and dissipation function, is given as

$$P_B^e = \frac{1}{2}\int_0^l \begin{Bmatrix} v'' \\ -w'' \end{Bmatrix}^T \begin{Bmatrix} M_{zz} \\ M_{yy} \end{Bmatrix} dx \tag{8}$$

At any instant of time, the generalized force vectors due to the bending action are obtained, in terms of nodal displacement vector and time derivatives, by utilizing the equation (6c) and equation (7) in (8), the bending energy expression. The stiffness, circulatory as well as damping matrices (which are commonly identified in a rotating system) may be obtained from the expression of generalized forces. The diagonal elements of bending moment expression give rise to direct elements (e.g. direct stiffness, direct damping matrix) whereas the off-diagonal elements give rise to cross coupled elements i.e. circulatory matrix. For an example the generalized force vectors in x-y and z-x plane for two layered rotor are given by

$$\begin{aligned} \{F\} = \begin{Bmatrix} \{F_{xy}\} \\ \{F_{zx}\} \end{Bmatrix} = &\left(\frac{a_{0_1} I_1}{b_{0_1} + b_{1_1} \mathrm{D}} + \frac{a_{0_2} I_2}{b_{0_2} + b_{1_2} \mathrm{D}}\right)[\mathrm{K_b}]\{\mathrm{q}\} + \Omega\left(\frac{a_{1_1} I_1}{b_{0_1} + b_{1_1} \mathrm{D}} + \frac{a_{1_2} I_2}{b_{0_2} + b_{1_2} \mathrm{D}}\right)[\mathrm{K_c}]\{\mathrm{q}\} \\ &+ \left(\frac{a_{1_1} I_1}{b_{0_1} + b_{1_1} \mathrm{D}} + \frac{a_{1_2} I_2}{b_{0_2} + b_{1_2} \mathrm{D}}\right)[\mathrm{K_b}]\{\dot{\mathrm{q}}\} \end{aligned} \tag{9}$$

The expression of $[K_b]$ and $[K_c]$ are given as

$$[K_b] = \int_0^l I\left[\phi''(x)\right]\left[\phi''(x)\right]^T dx, \qquad [K_c] = \int_0^l I\left[\phi''(x)\right]\begin{bmatrix} 0 & 1 \\ -1 & 0 \end{bmatrix}\left[\phi''(x)\right]^T dx, \quad \text{in}$$

which, $[\phi(x)]$, is the Hermite shape function matrix in x-y and z-x plane.

By incorporating these forces with the inertia forces, which are obtained from the expression of kinetic energy [14], the equation of motion for two layer rotor are given as

$$[M]\{\ddot{q}\}+[G]\{\dot{q}\}+\{F\}=\{P\} \tag{10a}$$

In the Eq.(10a) $\{P\}$ is the external nodal force vector, $[M]_{(8x8)}=[M_T]_{(8x8)}+[M_R]_{(8x8)}$, $[M_T]_{(8x8)}$ is the translational mass matrix, $[M_R]_{(8x8)}$ is the rotary inertia matrix, $[G]_{(8x8)}$ is the gyroscopic matrix. The expressions of translational mass matrix, rotary inertia matrix and gyroscopic matrix are given below after following [14].

$$[M_T]=\int_0^l \rho A\phi(x)\phi(x)^T\,dx,\ [M_R]=\int_0^l \rho I\phi'(x)\phi'(x)^T\,dx,\ [G]=\int_0^l 2\rho I\phi'(x)\begin{bmatrix}0 & 1\\ -1 & 0\end{bmatrix}\phi'(x)^T\,dx$$

where, A & I are the area & moment of inertia of the whole cross section.

After operating the operand on the nodal displacement vector and time derivatives, the equation of motion for constant angular speed is rewritten as.

$$[A_0]\{q\}+[A_1]\{\dot{q}\}+[A_2]\{\ddot{q}\}+[A_3]\{\dddot{q}\}+[A_4]\{\ddddot{q}\}=\{B\} \tag{10b}$$

where, $[A_0]=\left(a_{0_1}b_{0_2}I_1+a_{0_2}b_{0_1}I_2\right)[K_b]+\Omega\left(a_{1_1}b_{0_2}I_1+a_{1_2}b_{0_1}I_2\right)[K_c]$,

$[A_1]=b_{0_1}b_{0_2}[G]+\left(\left(a_{0_1}b_{1_2}I_1+a_{0_2}b_{1_1}I_2\right)+\left(a_{1_1}b_{0_2}I_1+a_{1_2}b_{0_1}I_2\right)\right)[K_b]+\Omega\left(a_{1_1}b_{1_2}I_1+a_{1_2}b_{1_1}I_2\right)[K_c]$,

$[A_2]=b_{0_1}b_{0_2}[M]+(b_{0_1}b_{1_2}+b_{0_2}b_{1_1})[G]+\left(a_{1_1}b_{1_2}I_1+a_{1_2}b_{1_1}I_2\right)[K_b]$,

$[A_3]=\left(b_{0_1}b_{1_2}+b_{0_2}b_{1_1}\right)[M]+b_{1_1}b_{1_2}[G]$,

$[A_4]=b_{1_1}b_{1_2}[M]$, $[B]=\left(b_{0_1}b_{0_2}+(b_{0_1}b_{1_2}+b_{0_2}b_{1_1})\mathrm{D}+b_{1_1}b_{1_2}\mathrm{D}^2\right)\{P\}$

It may be noted that the order of differential equations of motion depends on the number of viscoelastic layer as well as the material model.

4 RESULTS AND DISCUSSION

This section shows the numerical results to study the dynamic behavior of a two layered rotor-shaft system. The stability limit of spin speed (SLS) and steady state synchronous unbalance response amplitude (UBR) and time response have been obtained for two orientations of two layers.

4.1 The rotor shaft system

A simply supported two layered rotor shaft with two discs, as shown in the fig. 3(a), has been considered as an example. Fig. 3(b) shows the cross section of the shaft having two concentric layers of different materials of densities ρ_i and ρ_o. The radius ratio of the section and equivalent density are defined respectively as

$$\Re=\frac{r_i}{r_o},\qquad \rho=\rho_i\Re^2+\rho_o\left(1-\Re^2\right) \tag{11}$$

If the inner and outer materials are interchanged keeping the respective masses unchanged the radius ratio becomes

$$\Re' = \sqrt{1-\Re^2} \tag{12}$$

As $\Re \to 0$ the whole cross section is filled by the outer material of density ρ_o and $\Re \to 1$ signifies the cross section is made of inner material of density ρ_i. The radius ratios are used for finding out their effects and influences on the dynamics of a two layered rotor.

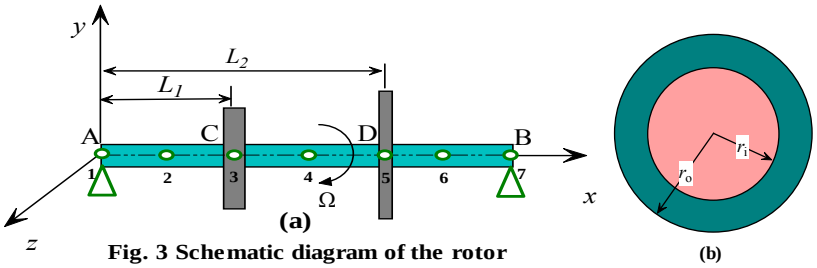

Fig. 3 Schematic diagram of the rotor

The materials forming the layers are assumed to be Poly-Vinyl-Chloride (PVC) and a polymer 'X' and the discs are assumed to be made of PVC. Following [15] the material properties of PVC at 24°C are taken as E = 4.0569e07 Pa, ρ = 1390 Kg/m^3 and the viscoelastic parameters in ADF approach are as B = 378.3029, C = 1.8591. The corresponding values for polymer 'X' at 75°**F** are E = 1.621e9 Pa, ρ = 1500 Kg/m^3, B = 430.411, C = 1.433 as given in [16]. The length and diameter of the rotor are 0.5 m, 0.05 m respectively. The disc dimensions are given in table (1) below.

	Outer diameter (m)	Thickness (m)	Mass unbalance (Kg m)	Node
Disc 1	0.15	0.030	10e-6	3
Disc 2	0.20	0.015	10e-6	5

Table 1: Disc parameters

4.2 The stability limit of spin speed and Campbell diagram

Stability Limit of the Spin speed (SLS) of the rotor–shaft system has been found out by plotting the maximum real part of all eigenvalues vs. spin speed. SLS corresponds to the spin speed when the maximum value of all real parts touches the zero line. The first natural frequency (FNF) is obtained by intersecting the imaginary part of first eigen value with the synchronous whirl ($\omega = \Omega$) line.

Fig. 4 shows the percentage increase of SLS and FNF for various radius ratios. Considering SLS and FNF the shaft performance is good when PVC is inside and polymer X forms the outside layer. This is obvious as polymer X is much stiffer than PVC and is placed outside. The SLS and FNF increase with radius ratio however after certain radius ratio, it decreases again. The equivalent

density increases with radius ratio. So there is a critical radius ratio for which maximum SLS and FNF can be achieved.

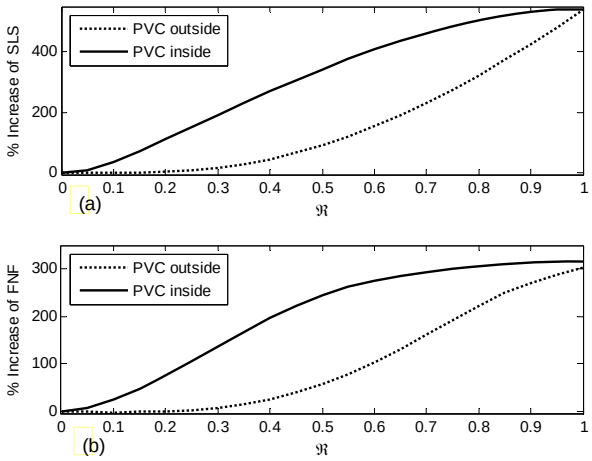

Fig. 4: Stability limit of spin speed and first natural frequency

The Campbell diagram of a rotating shaft is the plot between the eigen-frequency versus spin speed. Fig. 5 shows the Campbell diagram for different radius ratio when PVC is the inner layer. Only the forward and backward whirl for first displacement mode has been drawn. Due to gyroscopic effect the two whirl speed diverge at higher spin speed. It is seen from the figure that the value of eigen-frequency increases with high value of radius ratio.

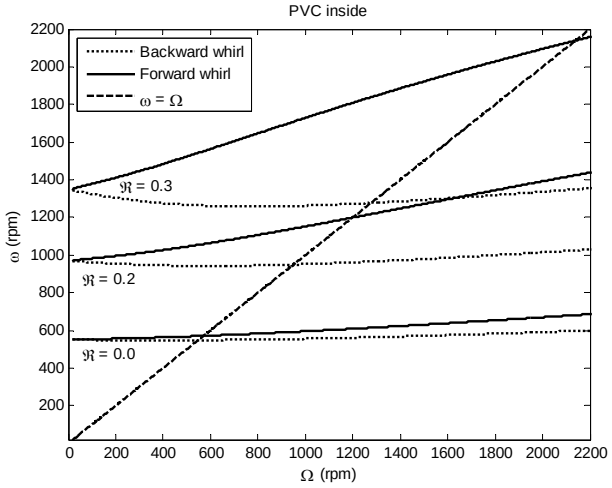

Fig. 5: The Campbell diagram

4.3 The synchronous unbalance response

The maximum real part of all eigenvalues vs. spin speed is plotted in fig.

6(a), for different radius ratios, keeping PVC as the inner layer. When it touches the zero line, the system becomes unstable and does not reach any steady state. It is seen from figure that the SLS as well as relative stability increase with increase in radius ratio as system becomes stiffer. Steady state synchronous Unbalance Response Amplitude (UBR) of the second disc is plotted in fig. 6(b) within the respective stable speed zones of operation (i.e. below the unstable zone marked by UZ). With increasing value of the radius ratio, the response amplitude decreases, as the shaft becomes stiffer.

Fig. 7 shows the time response of the second disc due to unbalance for two different radius ratios, when the rotor is assumed to rotate at about a speed of 1000 rpm. The rotor orbit is found to increase in amplitude monotonically for $\Re = 0.3$ and quenches for $\Re = 0.5$. This is due to the fact that spin speed in the first case is above, and in the second case, below the SLS.

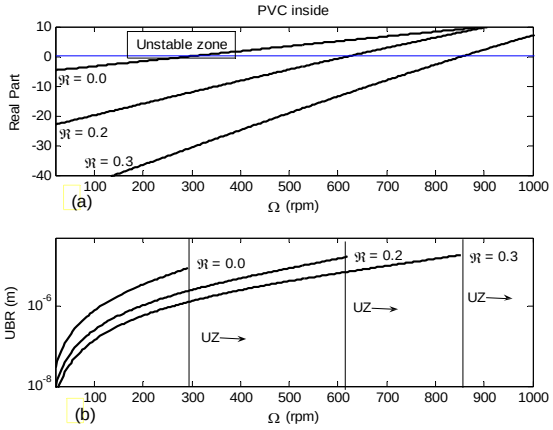

Fig. 6: UBR at second disc within stable zone

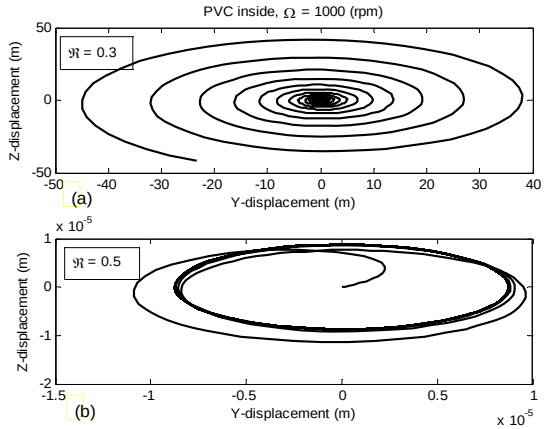

Fig. 7: Rotor orbit at the second disc

5 CONCLUSIONS

This paper reports a study of dynamics of rotors made of multilayered linearly viscoelastic materials. Building the equations of motion by taking into account the constitutive relationship of each layer in terms of a function of differential time operators forms the primary contribution. Finite element method is used to discretize the continuum. The material property or the constitutive relationship as well as the number of layers decide the order of the differential equations of motion. An eigen-analysis has been reported in this work, however, an important and interesting task of eigen-vector analysis or the analysis of modes demands careful attention particularly for higher order problems as in this case. The layers should be arranged in the order of increasing stiffness from inside to outside. The results show, that optimum values of thickness of different layers, as well as their placements are important; hence an optimization technique may be used for a given purpose. Lastly the inspiration for using the multilayered architecture and the associated formulation is obtained by appreciating the importance of light, yet sufficiently strong rotor-shafts, at least for the cold working environments.

REFERENCES

[1] Nakra B.C., "*Vibration Control in Machines and Structures using Viscoelastic Damping*", Journal of Sound and Vibration, vol. 211(3)., pp. 449-465, 1998.

[2] Bland D.R., "*Linear Viscoelasticity*", Pergamon Press, Oxford, 1960.

[3] Lesieutre G.A. and Mingori D.L., "*Finite Element Modelling of Frequency-Dependent Material Damping Using Augmenting Thermodynamic Fields*", AIAA Journal of Guidance, Control and Dynamics, vol. 13(6)., pp. 1040-1050, 1990.

[4] Lesieutre G.A., Bianchini E. and Maiani A., "*Finite Element Modelling of One-Dimensional Viscoelastic Structures Using Anelastic Displacement Fields,*" Journal of Guidance and Control, vol. 19(3)., pp. 520-527, 1996.

[5] Dimentberg M., "*Flextural Vibration of Rotating Shafts*", Butterworth, London, England, 1961.

[6] Tondl A., "*Some Problems of Rotor Dynamics*", Prague Publishing House of Czechoslovak Academy of Sciences, pp. 17-69, 1965.

[7] Genta G., "*Dynamics of Rotating Systems*", Springer Verlag, 2005.

[8] Zorzi E.S. and Nelson H.D., "*Finite Element Simulation of Rotor-bearing Systems with Internal Damping*", Journal of Engineering for Power, Transactions of the ASME, vol. 99., pp. 71-76, 1977.

[9] Ozguven H.N. and Ozkan Z.L., "*Whirl Speeds and Unbalance Response of Multibearing Rotors Using Finite Elements*", Journal of Vibration, Acoustics, Stress, and Reliability in Design, Transactions of the ASME, vol. 106., pp. 72 -79, 1984.

[10] Grybos R., "*The Dynamics of a Viscoelastic Rotor in Flexible Bearing.*" Archive of Applied Mechanics, Springer Verlag, vol. 61., pp. 479-487, 1991.
[11] Roy H., Dutt J.K. and Datta P.K., "*Dynamics of a Viscoelastic Rotor Shaft Using Augmenting Thermodynamic Fields — a Finite Element Approach*", International Journal of Mechanical Sciences, vol. 50., pp. 845-853, 2008.
[12] Friswell M.I., Dutt J.K., Adhikari S. and Lees A.W., "*Time domain analysis of a viscoelastic rotor using internal variable models*", vol. 52., pp. 1319–1324, 2010.
[13] Dutt J.K. and Roy H., "*Viscoelastic Modelling of Rotor-Shaft Systems using an operator based approach*", Journal of Mechanical Science, IMechE, Part-C, vol. 224., pp. 73-87, 2011.
[14] Rao J.S., "*Rotor Dynamics*", New Age International Publishers, 1996.
[15] Roy H., "*Study of Dynamics of Viscoelastic Rotors-A Finite Element Approach*", Ph.D. Thesis from Indian Institute of Technology, Kharagpur, India, June 2008.
[16] Roy H., Dutt J.K., Datta P.K., "*Dynamic Behaviour of a Viscoelastic Beam using ATF and ADF – A Finite Element Approach*", Accepted for publication in the Advances in Vibration Engineering Journal, 2011.